Ellipsometric Characterization of Rubbed Polyimide Alignment Layer in Relation with Distribution of Liquid Crystal Molecules in Twisted Nematic Cell

Sung Yong Cho[1], Sang Uk Park[2], Sung Mo Yang[1], and Sang Youl Kim[1,2]*

[1]*Department of Physics, Ajou University, Suwon 16499, Korea*
[2]*Ellipso Technology Co., Ltd., Suwon 16498, Korea*

Ultra-small optical anisotropy of a rubbed polyimide (PI) alignment layer is quantitatively characterized using the improved reflection ellipsometer. Twisted nematic (TN) cells are fabricated using the rubbed PIs of known surface anisotropy as alignment layers. Distribution of liquid crystal (LC) molecules in the TN cell is characterized using transmission ellipsometry. The retardation of the rubbed PI surface increases as rubbing strength increases. The tilt angle of the optic axis of the rubbed PI surface decreases as rubbing strength especially as the angular speed of the rubbing roller increases. Pretilt angle of LC molecules in the TN cell shows strong correlation with tilt angle of the optic axis of the rubbed PI surface. Both the apparent order parameter and the effective twist angle of the LC molecules in the TN cell decrease as the pretilt angle of LC molecules increases.

Keywords : Rubbed polyimide, Optical anisotropy, Distribution of liquid crystal, Ellipsometry
OCIS codes : (240.2130) Ellipsometry and polarimetry; (230.3720) Liquid-crystal devices; (260.1440) Birefringence; (160.1190) Anisotropic optical materials

I. INTRODUCTION

The alignment layer as one of the main elements constituting a liquid crystal display (LCD), plays an important role in maintaining reliable orientation of liquid crystal (LC) molecules [1]. The contribution of the alignment layer to the major optical properties of the LCD is well realized by regulating the molecular distribution of LCs through the surface anchoring on the layer [1-4]. Many techniques such as photo-alignment [5], oblique evaporation [6], formation of Langmuir-Blodgett films [7] and rubbing surfaces [8, 9] are developed to form alignment layers. The technique of rubbing polyimide (PI) has been widely used in the LCD industry by virtue of its strong anchoring energy and cost effectiveness for mass production. To improve the picture quality of the LCD, many research efforts have been concentrated on the effects of the rubbing process together with its variables. In order to characterize the rubbed PI alignment layer itself, those techniques like

atomic force microscopy (AFM) [10], polarimetry and ellipsometry [8, 11, 12], near edge X-ray absorption fine structure spectroscopy [13], surface lamellar decoration, surface enhanced Raman scattering, and second harmonic generation [14], have been introduced. Among the above-mentioned techniques, AFM has the advantage of scanning detailed morphology of rubbed PI surfaces, but it has the disadvantages such that it takes a long time to measure a large-sized sample and the probing tip can damage the surface of the sample. Optical techniques have the advantages of being fast and non-contact, but it is very difficult to detect and characterize the ultra-small optical anisotropy of a rubbed PI alignment layer quantitatively. Conventional ellipsometers used to characterize the ultra-small optical anisotropy of rubbed PI show the limitation that both the retardation and the tilt angle of rubbed PI are not measured accurately [11, 12]. When the retardation is measured with accuracy, the tilt angle is not measured at all [8]. Thus the direct relation between the anisotropic property of an

Color versions of one or more of the figures in this paper are available online.

alignment layer and the distribution of LC molecules has rarely been reported. Meanwhile, Seo *et al*. reported that the polymer tilt angle, which is defined as the incident angle of minimum optical retardance, is not related directly to the pretilt angle of LC molecules [15]. Recently, improved ellipsometers which demonstrated resolution of 0.002 nm in retardation measurement have been developed [18, 19], and these ellipsometers have been utilized for quantitative characterization of the ultra-small optical anisotropy of rubbed PI surfaces [16-19].

In this research, the ultra-small optical anisotropy of a series of rubbed PI surfaces is quantitatively addressed using the improved reflection ellipsometer. Special efforts are exerted to keep the sample stage wobble-less, which results in precise determination of the tilt angle of the rubbed PI surface. Twisted nematic (TN) cells are fabricated using the rubbed PIs of known surface anisotropy as alignment layers. Distribution of liquid crystal (LC) molecules in the TN cell is characterized using transmission ellipsometry. The key variables which relate the optical anisotropy of rubbed PI surface to the parameters describing distribution of LC molecules in the TN cell is investigated.

II. SAMPLE PREPARATION AND MEASUREMENT

2.1. PI Alignment Layer

Corning-7059 (Corning Co., Ltd., USA) glass of $30 \times 30 \times 0.7$ mm^3 in size is used as a substrate. PI (AL22620, JSR Co., Ltd., Japan) is spin-coated on the glass substrate at 4000 rpm for 40 seconds, and it is dried at 80°C for 1 min and then annealed at 220°C for 15 min using a hotplate. The thickness of PI layers is measured using a spectroscopic ellipsometer (Elli-SE, Ellipso Technology Co., Korea), and it ranged from 120 nm to 140 nm. To get an alignment layer, the PI layer on glass is rubbed using a rubbing machine (RMS, NAMIL Co., Korea) where i) the penetration depth of the rayon fabric (YA-181-RN, MRC Co., Korea) is varied from 0.35 mm to 0.40 mm, and ii) the angular speed of the roller is set at 250, 500, 1000, or 2000 rpm. The roller radius and the stage speed are set at 60 mm, and 33.3 mm/s, respectively. For a fast and precise characterization of the ultra-small anisotropy of the rubbed PI surface, the improved reflection ellipsometer (Elli-AAL, Ellipso Technology Co., Korea) operating at the incident angle of 35° and at the wavelength of 450 nm is used [20]. About 140 ellipsometric data points are collected while the sample stage is being rotated 360° in 11 seconds.

2.2. Twisted Nematic (TN) Cells

TN cells are fabricated by dropping the UV-curing epoxy (NOA65, Norland Product Inc., USA) mixed with calibrated glass-bead spacers (diameter is ~5.53 μm) on corners of the rubbed PI layer on glass, and then by covering it with another rubbed PI layer with its rubbing direction making a right angle with that of the bottom PI layer. Two PI alignment layers with similar optical anisotropy are chosen as a pair for each TN cell. The cell gap of the TN cell is monitored using a reflection spectrometer, and its local variation is minimized by pressing down the large cell gap area with a spatula. When the cell has a uniform gap, the epoxy is exposed with an unpolarized UV light ($\lambda = 365$ nm) using a UV lamp (UV.LF104L, UVItec, UK). Nematic LC (MDA-99-3996, Merck Co., Germany) is filled into the cell by a capillary action and the cell is baked in an oven for 60 min at 100°C. For a determination of the molecular distribution of LC molecules in the TN cell, a transmission ellipsometer with customized stage of tilt and rotation (Elli-RET, Ellipso Technology Co., Korea) operating at the wavelength of 550 nm is used [20]. With this customized sample stage, ellipsometric data can be collected continuously while the sample is being rotated at its tilted position [20-22]. In the present work, the sample is tilted such that the incident angle is varied from 0° to 50° at an interval of 10°. At each incident angle, the transmission ellipsometric data are continuously collected while the sample is being rotated 360°.

III. THEORY AND ANALYSIS

The ellipsometer is an optical instrument commonly applied to analyze the structure and the optical properties of multilayered samples. The measured quantities are the phase difference ($\triangle$) and the amplitude ratio ($\tan\psi$) between p- and s-polarized light of either the transmitted light through a sample or the reflected light from a sample surface [23, 24]. For a rotating analyzer type ellipsometer, the Fourier coefficients (α, β) of measured intensity I_D are related with ellipsometric constants (ψ, $\triangle$) as follow [23].

$$I_D = I_0(1 + \alpha\cos 2\omega t + \beta\sin 2\omega t)$$

$$\alpha = \frac{\tan^2\psi - \tan^2 P}{\tan^2\psi + \tan^2 P}$$

$$\beta = \frac{2\tan\psi\cos\triangle\tan P}{\tan^2\psi + \tan^2 P} \tag{1}$$

where ω is the angular frequency of the rotating analyzer and P is the azimuth angle of the polarizer. Measured Fourier constants (α, β) contain information of optical property and layer structure of the sample of interest.

3.1. Characterization of Rubbed PI Alignment Layer

It has been suggested by previous researchers that a rubbed PI can be optically described using the model composed of a molecule-orienting upper layer and a random lower layer [11, 12]. Thus the optical model used in this work for analysis of the rubbed PI sample is the two layer

system composed of a uniaxially anisotropic upper layer and an isotropic lower layer. The detailed expressions of ellipsometric constants (α, β) for analysis of the samples with anisotropic layers can be found elsewhere [25, 26]. The best fit calculated ellipsometric constants to the measured ones are searched to determine model parameters. Using such determined model parameters, optical anisotropy of the rubbed PI layer is expressed in terms of i) azimuth angle and tilt angle of the optic axis ii) birefringence and thickness, of the uniaxial upper layer. Retardation is obtained by multiplying birefringence with the upper layer thickness in nm.

3.2. Characterization of the Molecular Distribution of LC in a TN Cell

The optical model for the analysis of distributed LC molecules in a TN cell is similar to the model used for the analysis of discotic LC molecules in a wide-view film [21, 22]. In the present work, it is assumed that LC molecules in a TN cell can be optically replaced by 50 uniform sublayers (Fig. 1), where the birefringence and the pretilt angle of each sublayer are the same. The azimuth angle of the sublayers is assumed to increase linearly from the bottom sublayer to the top one (Fig. 2).
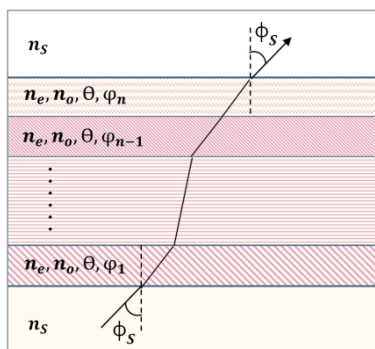

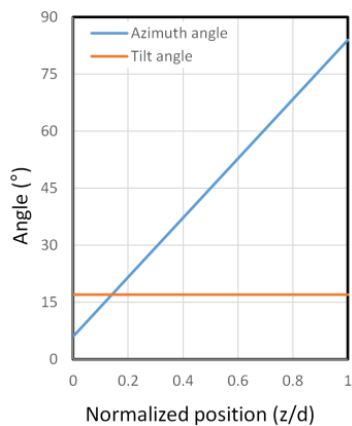FIG. 1. The optical model used to represent the distribution of LC molecules in TN cell.

FIG. 2. Suggested director distribution of LC molecules in TN cell along z-coordinate.

Measured ellipsometric data at six different incident angles are handled as a single data set in the modelling process of determining model parameters. Using the determined model parameters, distribution of LC molecules in the TN cell is described in terms of pretilt angle, twist angle (difference between the azimuth angle of the top sublayer and that of the bottom one) and birefringence of LC sublayers. Retardation can be obtained by multiplying birefringence with cell gap (the total thickness of 50 sublayers) in nm.

3.3. Investigation of the Relation between Surface Anisotropy of Rubbed PI and LC Distribution in TN Cell

The relation between the parameters representing the anisotropic property of rubbed PI alignment layers and those representing the distribution of LC molecules in the TN cell is investigated. The parameters representing the anisotropic property of the rubbed PI surface consist of retardation, the tilt angle and the azimuth angle of the upper uniaxial layer. Birefringence, the pretilt angle and the twist angle of LC molecules are the parameters representing LC distribution in the TN cell. Only those parameters which show explicit correlation or explicit anti-correlation are reported in this manuscript in relation with the corresponding rubbing variable.

IV. RESULTS AND DISCUSSION

4.1. Rubbed PI Alignment Layer - Magnitude and Direction of Uniaxial Surface Anisotropy

Typical curves of measured (α, β) of a rubbed PI on glass substrate are shown in Fig 3. Either α or β of the rubbed PI with an anisotropic surface layer shows an oscillatory behavior versus azimuth angle of the sample. If the surface of a rubbed PI is uniaxially anisotropic with its optic axis directed parallel to the surface (zero tilt angle), then the oscillation becomes a sinusoidal one with a period of 180°. The amplitude of this sinusoidal variation is proportional to the magnitude of the uniaxial anisotropy. The maximum (or minimum) position of this oscillation indicates the azimuth angle of the optic axis. Due to the ultra-small optical anisotropy of the rubbed PI surface, the amplitude of this oscillation is very small, ranging from 0.001 to 0.003 as shown in Fig. 3. Thus the ellipsometric constants (α, β) are collected with the precision better than 1.0×10^{-4}. When the tilt angle of the optic axis is not zero, a distortion from the ideal sinusoidal one occurs, and hence analyzing the distortion from the ideal sinusoidal oscillation, one can determine the tilt angle of the optic axis. Since even a very small wobble of sample surface will inevitably introduce an artificial oscillation and an additional distortion into (α, β), a special effort is paid by the authors to keep the wobble of the sample surface below 0.001°. A detailed explanation of the improved ellipsometer
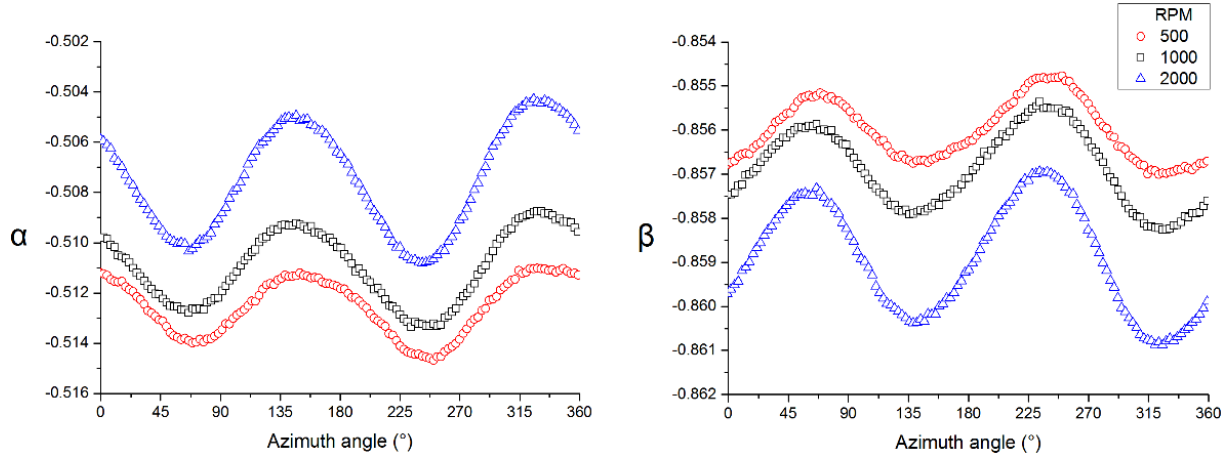
FIG. 3. Measured ellipsometric constant (α or β) of a rubbed PI on glass substrate shows an oscillatory behavior versus the azimuth angle of sample. Amplitude of this oscillation increases as the angular speed of the rubbing roller increases from 500 rpm ($\circ$) to 2000 rpm ($\triangle$). The distortion from an ideal sinusoidal oscillation comes from a non-zero tilt angle of the optic axis of the upper uniaxially anisotropic layer.

which enables high precision measurement with near zero wobble, and the modelling analysis of the distorted sinusoidal oscillation can be found elsewhere [18-20]. The modelling analysis of the measured (α, β) curves are carried out as explained in the previous section, using the optical model of a uniaxially anisotropic upper layer on top of an isotropic lower layer.

Determined model parameters of rubbed PI samples are summarized as follow. The average thickness of unrubbed PIs is about 130 nm, which decreases to about 100 nm after rubbing. The uniaxially anisotropic upper layers have about 50 nm of average thickness, 1.534 of average refractive index, and 0.004~0.011 of birefringence. The refractive index of the glass substrate is fixed at the measured value of $n = 1.532$ by using a spectroscopic ellipsometer. In Fig. 4, rubbing strength dependence of retardation of the rubbed PI is presented. Retardation of the rubbed PI surface increases as either the angular speed of the rubbing roller or the rubbing depth increases. It increases from 0.22 nm

to 0.35 nm as the angular speed of the rubbing roller increases from 250 rpm to 2000 rpm (stage speed is 33 mm/s and rubbing depth is 0.4 mm). At the rubbing depth of 0.35 mm, it shows similar increasing behavior versus angular speed but the average retardation is smaller. Increase of retardation comes from increase of both birefringence and thickness of the anisotropic upper layer. These observations are in accordance with previous reports on the retardation or the anchoring energy of rubbed PIs versus rubbing strength [8, 9].

Tilt angle and azimuth angle of the optic axis of the rubbed PI surface are determined also, simultaneously with the retardation through modelling analysis. Tilt angle decreases from 11.5° to 6.0° as the angular speed of the rubbing roller increases from 250 rpm to 2000 rpm (rubbing depth is 0.40 mm) as shown in Fig. 5. This result is not in accordance with the report that tilt angle is not related directly with rubbing strength [15]. It should be noted that in the present work, wobble of the sample surface is
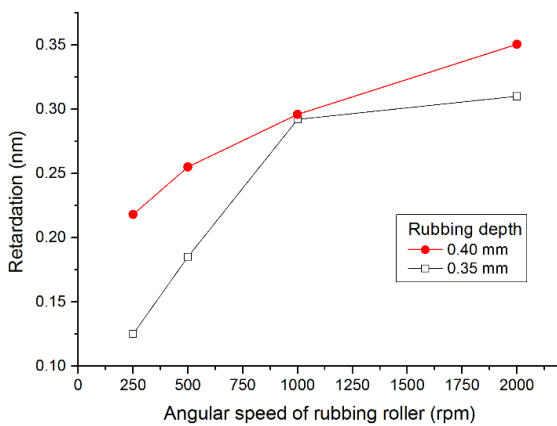

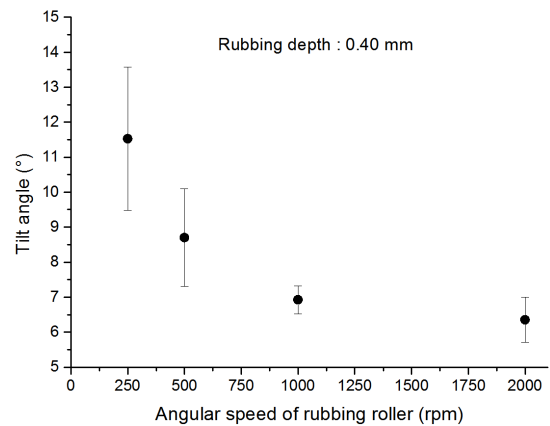FIG. 4. Retardation of rubbed PIs versus the angular speed of the rubbing roller.

FIG. 5. Tilt angle of the optic axis of rubbed PI decreases as the angular speed of rubbing roller increases.

suppressed below 0.001°, and hence the artificial distortion of the measured (α, β) which could be introduced from wobbling of the sample surface is suppressed to almost zero. The authors believe that the observed oscillation together with the observed distortion of the measured (α, β) from an ideal sinusoidal one, is entirely caused by the tilted optic axis of the rubbed PI surface. Definitely, tilt angle of the optic axis of the rubbed PI surface depends on the angular speed of the rubbing roller, at least for the PI (AL22620, JSR Co., Ltd., Japan) used in this experiment. It decreases as the rubbing strength increases [27, 28], and apparently the angular speed of the rubbing roller is the dominant element of rubbing strength which affects tilt angle.

On the other hand, the azimuth angle does not show any noticeable variation versus rubbing variables. The measured values are scattered around 133.4°.

4.2. Distribution of LC Molecules in TN Cell

The measured variation of ellipsometric constants of LC filled TN cells versus sample azimuth angle is analyzed, and the model parameters describing the distribution of LC molecules in TN cells are obtained. Since retardation of a LC filled TN cell is much greater than that of a rubbed PI alignment layer, anisotropy of the alignment layer including the residual anisotropy of the glass substrate is neglected in this analysis.
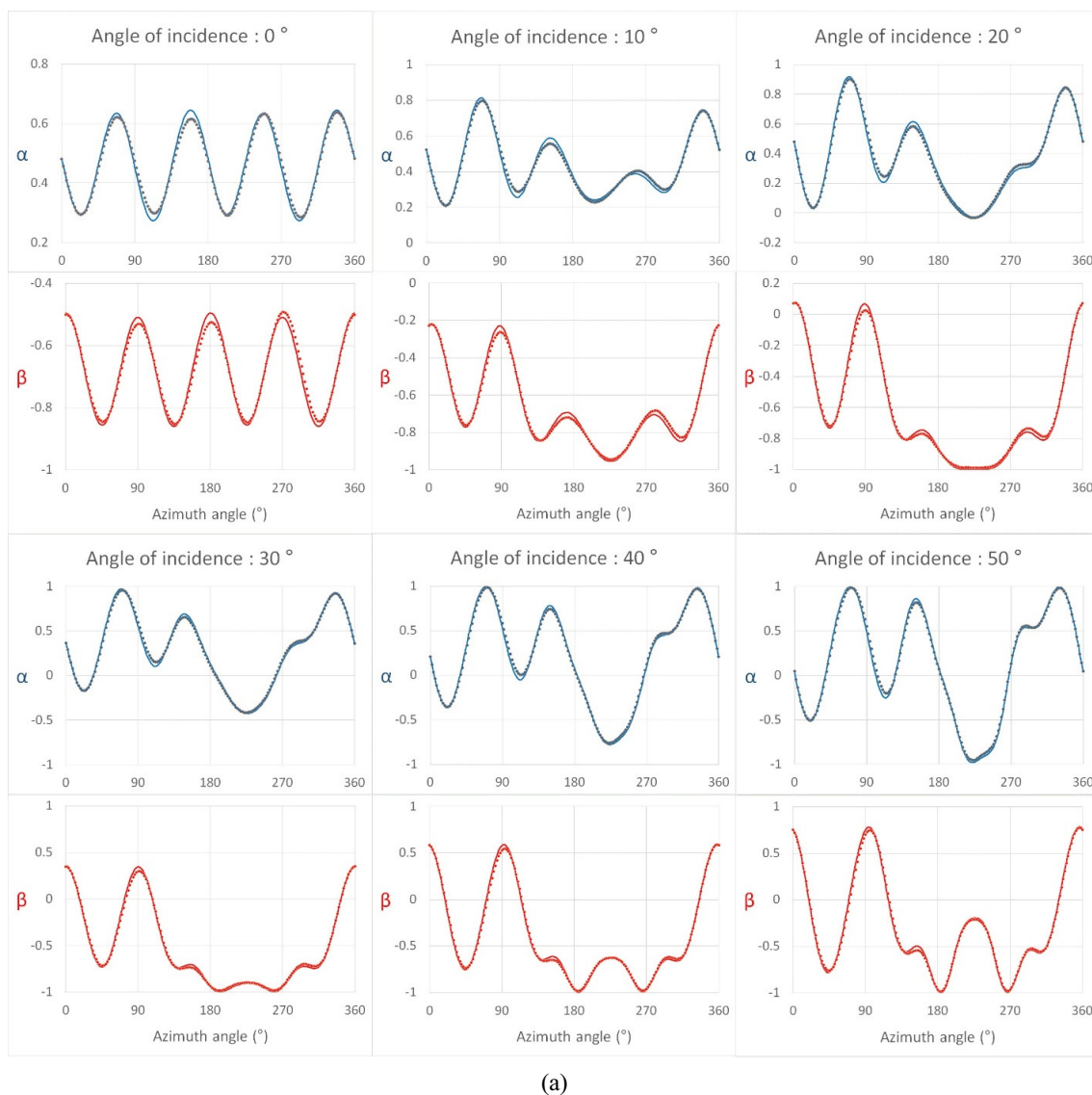

(a)

FIG. 6. (a) Comparison of measured (dots) ellipsometric constants (α, β) of a TN cell with the best fit (solid lines) ones for six incident angles from 0° to 50°. The pretilt angle of LC molecules is 17.3°, the twist angle is 83.2°, the cell gap is 4.74 μm, and birefringence is 0.136. As the incident angle increases from 0°, the sinusoidal variation gets distorted immediately, and the distortion becomes more severe at greater incident angles. (b) The simulated ellipsometric constants (α, β) of the TN cell for zero pretilt angle. Other parameters are kept the same. The distortion also appears at non-zero incident angles, but it is less severe and the oscillation conserves 180° period.

Ellipsometric constants (α, β) versus azimuth angle of a TN cell show quite drastic variations as i) either the cell gap (the total thickness of LC sublayers) of a TN cell or birefringence of LC sublayers, ii) either the twist angle or the pretilt angle of LC molecules and iii) the incident angle, are varied. As a typical example, measured ellipsometric constants of a TN cell together with the best fit ones are presented in Fig. 6(a). When the incident angle is 0°, either α or β shows a sinusoidal oscillation versus sample azimuth angle with a period of 90°. The amplitude of this oscillation is proportional to the in-plane retardation of cell. As incident angle increases, the sinusoidal variation gets distorted immediately, and this distortion becomes

more severe both at greater pretilt angles of LC molecules and at greater incident angles. The pretilt angle of LC molecules in the TN cell shown in Fig. 6(a) is 17.3°. Distortion from the sinusoidal oscillation still exists even when the pretilt angle of LC molecules is zero, if incident angle is not 0°. But this distortion which appears at the pretilt angle of 0° is less severe and the oscillation is semi-sinusoidal with the period of 180° (Fig. 6(b)).

When the twist angle, defined as the difference between the azimuth angle of the top sublayer and that of the bottom sublayer (Fig. 2), is changed, the sinusoidal oscillation of ellipsometric constants (α, β) versus azimuth angle is distorted quite drastically also, but in a different pattern
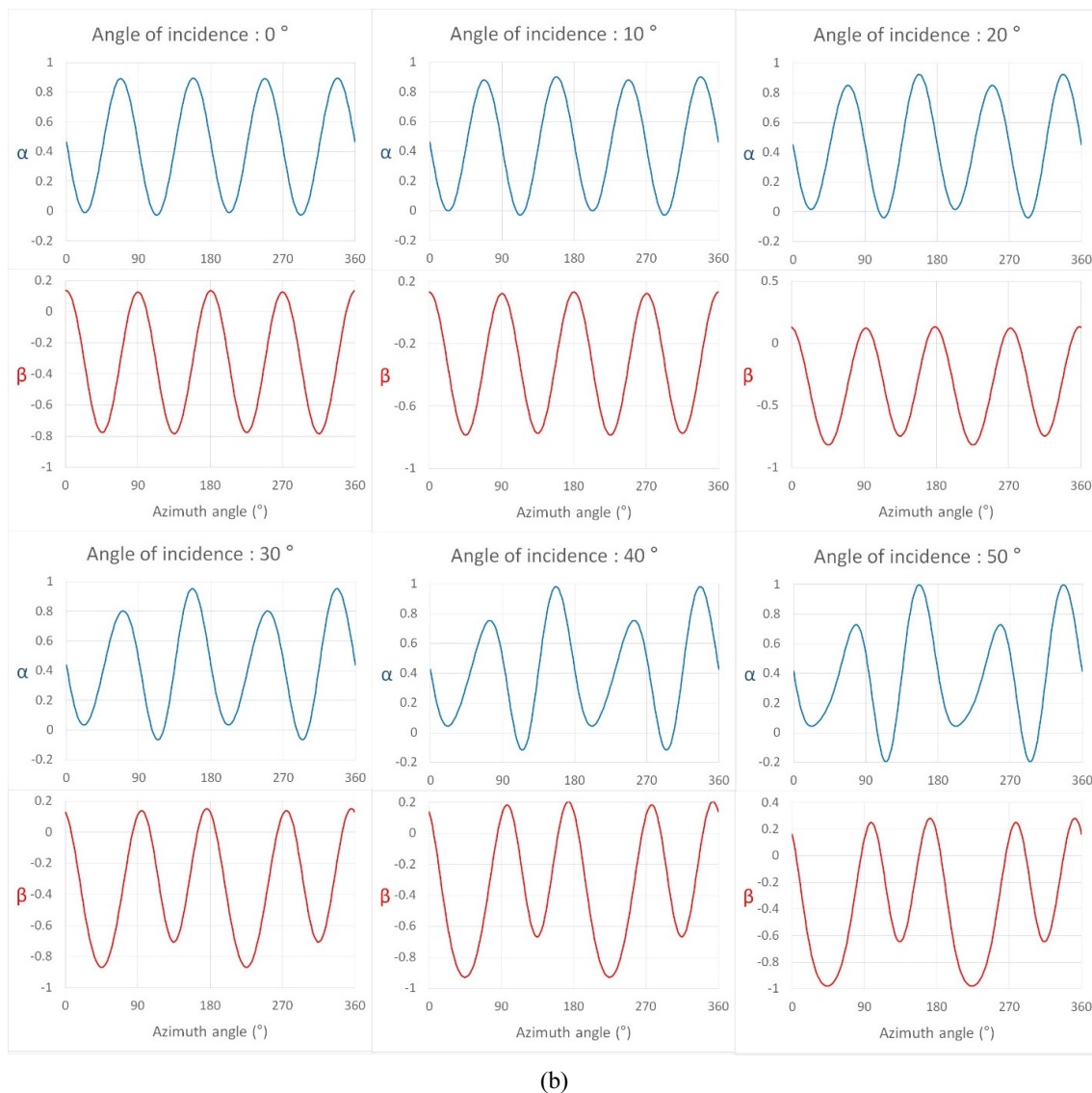

(b)

FIG. 6. (a) Comparison of measured (dots) ellipsometric constants (α, β) of a TN cell with the best fit (solid lines) ones for six incident angles from 0° to 50°. The pretilt angle of LC molecules is 17.3°, the twist angle is 83.2°, the cell gap is 4.74 μm, and birefringence is 0.136. As the incident angle increases from 0°, the sinusoidal variation gets distorted immediately, and the distortion becomes more severe at greater incident angles. (b) The simulated ellipsometric constants (α, β) of the TN cell for zero pretilt angle. Other parameters are kept the same. The distortion also appears at non-zero incident angles, but it is less severe and the oscillation conserves 180° period (Continued).

[27, 28]. Thus the shape and magnitude of the distorted sinusoidal oscillation contains ample information to describe the distribution of LC molecules in the TN cell. It is confirmed by the authors that ellipsometric constants (α, β) versus the sample azimuth angle at incident angles from 0° to 50° provide excellent sensitivity to determine unambiguously model parameters which describe the distribution of LC molecules in the TN cell.

Elaborate fitting procedure to the measured ellipsometric constants (α, β) at incident angles from 0° to 50°, is executed and the model parameters describing the distribution of LC molecules in the TN cell are determined. The fit of the calculated ellipsometric constants (α, β) to the measured ones is quite excellent as shown in Fig 6(a), for an example. The best fit model parameters of the sample in Fig. 6(a), are the pretilt angle of 17.3°, the twist angle of 83.2°, the cell gap of 4.74 μm, and birefringence of 0.136.

4.3. Relation between Anisotropy Parameters of a Rubbed PI Surface and Parameters of LC Distribution in a TN Cell

The determined model parameters describing the anisotropic characteristics of rubbed PI surfaces and those parameters describing the distribution of LC molecules in the corresponding TN cell, are summarized into Table 1. The cell gap ranges from 4.62 μm to 4.94 μm. The average refractive index of the LC layer is 1.561, and birefringence of LC layer ranges from 0.066 to 0.136. For further analysis, the averaged tilt angle of the top rubbed PI and the bottom rubbed PI is used as the tilt angle of the rubbed PI. As mentioned above, the twist angle of LC in the TN cell (in Table 1) is obtained by taking the difference between two azimuth angles of top sublayer and bottom sublayer. In order to compensate the effect of small variation of the azimuth angle of rubbed PIs to the twist angle of LC in the TN cell, the effective twist angle
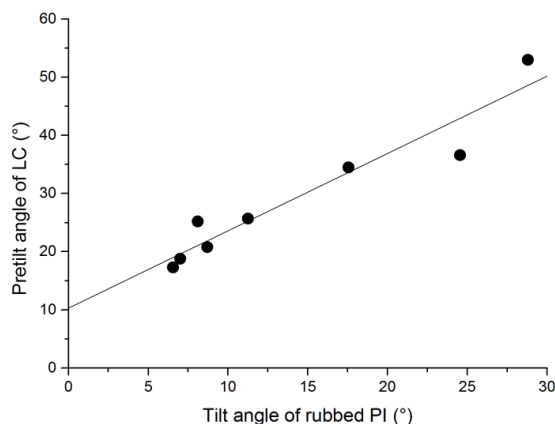

FIG. 7. The pretilt angle of LC molecules in the TN cell increases linearly with the tilt angle of rubbed PI.

of the LC layer which is obtained by adding the azimuth angle difference between the top rubbed PI and the bottom PI to the twist angle of corresponding LC in the TN cell, is introduced.

After a close investigation of the numbers in Table 1, one can find that the pretilt angle of LC molecules in the TN cell increases almost linearly with the tilt angle of the rubbed PI (Fig. 7). The slope and the y-intersection of the line in Fig. 7 are 1.33 and 10.3°, respectively. Considering that the tilt angle of the rubbed PI decreases as the rubbing strength increases, it is easily predictable that the pretilt angle of LC molecules can be manipulated by controlling the rubbing strength. Since the angular speed of the rubbing roller is identified as the dominant element of the rubbing strength, it can be usefully applied in controlling the tilt angle of the rubbed PI and thus to manipulate the pretilt angle of LC molecules. The pretilt angle of LC molecules will decrease as the angular speed of the rubbing roller increases. Even though, as is implied by the nonzero y-intersection in Fig. 7, the pretilt angle of

TABLE 1. Summary of model parameters describing the surface anisotropy of rubbed PI layers and the distribution of LC molecules in TN cell

Sample #	Rubbed PI (top)			Rubbed PI (bottom)			LC in TN cell			
	Retardation (nm)	Azimuth angle (°)	Tilt angle (°)	Retardation (nm)	Azimuth angle (°)	Tilt angle (°)	Birefringence (Δn)	Pretilt angle (°)	Twist angle (°)	Cell gap (μm)
1	0.321	135.1	7.4	0.318	137.4	6.6	0.126	18.8	80.0	4.71
2	0.223	135.9	9.0	0.230	137.8	8.4	0.135	20.8	82.1	4.71
3	0.161	136.9	9.2	0.152	136.6	13.3	0.133	25.7	81.1	4.77
4	0.402	133.4	7.1	0.414	131.7	6.0	0.136	17.3	83.2	4.74
5	0.193	132.2	14.5	0.193	134.2	20.6	0.066	34.5	76.8	4.94
6	0.211	135.2	7.2	0.220	137.3	9.0	0.113	25.2	78.7	4.62
7	0.223	131.8	25.3	0.209	132.5	23.8	0.097	36.6	77.9	4.77
8	0.133	135.8	26.9	0.147	129.4	30.7	0.108	53.0	76.2	4.91

the LC molecules will remain nonzero even when the angular speed is increased by a great amount.

The LC molecule used in this work is a uniaxial one and the anisotropic refractive indices provided by the supplier are $n_e = 1.6307$ and $n_o = 1.4984$. When LC molecules are randomly oriented in a cell, the cell is optically isotropic. Both the birefringence of the cell and the order parameter of LC layer are zero. If LC molecules are aligned, depending on the degree of alignment, birefringence of the LC layer will increase from zero to its maximum value of Δn_{max}. The order parameter defined as $S = \langle 3\cos^2\theta - 1\rangle/2$ will also increase from 0 to 1. One can find many reports trying to define the order parameter as a linear function of either birefringence or the anisotropy of molecular polarizability [29-33]. A quite recent research work based on an extensive numerical calculation of the relation between the order parameter and birefringence of a series of aligned LC molecules, revealed that the order parameter S can be approximated from the measured birefringence using the following equation [34, 35].

$$S = (1 + a)\triangle n_{rel} - a\triangle n_{rel}^2 \qquad (2)$$

where $a = \dfrac{1}{4}n_o\triangle n_{max}$ and $\triangle n_{rel}$ is the relative birefringence defined as the measured birefringence (Δn) divided by Δn_{max}.

LC molecules in an anti-parallel cell may distribute uniformly and the order parameter will be position independent. LC molecules in a TN cell would distribute twistedly, or non-uniformly. Even if the director is gradually twisted from top to bottom, the order parameter of LC molecules in a TN cell can be calculated from the relative birefringence. Meanwhile, if the measured anisotropic refractive indices of $n_e = 1.6307$ and $n_o = 1.4984$ is obtained when LC molecules are not ideally aligned, the calculated order parameters using $\Delta n_{max} = 0.1323$ will be the relative one and it will represent the relative ordering of LC molecules compared to that of the LC molecules configured by the supplier. The calculated order parameter may not be the absolute one and hence the word of *apparent order parameter* will be used in this manuscript. The apparent order parameter of the LC layer in the TN cell is calculated using the measured birefringence of the LC layer in the TN cell (Table 1) and Eq. (2). The apparent order parameter shows a strong anti-correlation with the pretilt angle of LC molecules (Fig. 8). This observation is in accordance with the understanding that LC molecules will align better when rubbing strength is increased. As rubbing strength is increased, the tilt angle of the rubbed PI and the pretilt angle of LC molecules decrease, and LC molecules tend to align better. The apparent order parameter is around 1 for smaller pretilt angles and decreases rapidly as the pretilt angle increases. Considering that it is very hard to get perfectly aligned LC molecules under an ordinary environment, the value of 1 as the apparent order parameter may simply mean that the degree of ordering achieved in this

work is comparable with that of the supplier who provided the anisotropic refractive indices of this LC molecule. The experimentally determined birefringence of the LC layer which exceeds Δn_{max} leads to greater apparent order parameters than 1.

When LC molecules anchor strongly on the surface of alignment layers and the top alignment layer makes a right angle with the bottom one, then the twist angle of LC molecules in the TN cell will be 90°. The effective twist angles determined in this work are smaller than 90°. Smaller effective twist angles than 90° are understood as originating from the not-so-strong anchoring. Thus, the deviation of effective twist angle from 90° can be used as a measure of weakening of surface anchoring strength. The variation of the effective twist angle versus the pretilt angle of the LC layer in the TN cell is shown in Fig. 9. The effective twist angle decreases almost linearly to the pretilt angle, which indicates the LC molecules of larger pretilt angle have weaker anchoring strength. The y-intersection in Fig. 9 is the same as the ideal effective twist angle of 90°, which could be achieved if the pretilt angle were 0°.
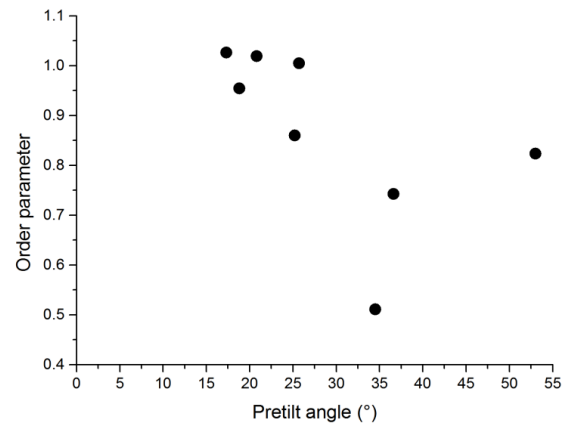

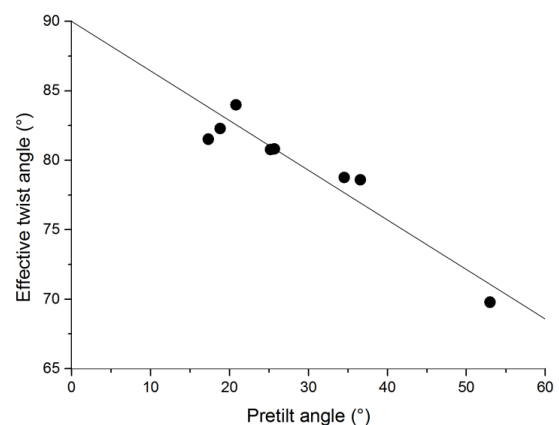FIG. 8. The apparent order parameter of LC layer in TN cell decreases as the pretilt angle of LC molecules increases.

FIG. 9. The effective twist angle versus the pretilt angle of LC molecules in TN cell.

V. CONCLUSION

Using the improved reflection ellipsometer, ultra-small optical anisotropy of rubbed PI surfaces is quantitatively characterized. Retardation of rubbed a PI surface increases as either rubbing depth or the angular speed of the rubbing roller increases. The tilt angle of the optic axis of the rubbed PI surface decreases as rubbing strength increases. The angular speed of the rubbing roller appears to be the dominant element of the rubbing strength. TN cells are made using the rubbed PI samples of known optical anisotropy as alignment layers. The distribution of LC molecules in TN cell is characterized using trans- mission ellipsometry. The results are given in terms of the pretilt angle, the twist angle, birefringence of LC layer in the TN cell and the cell gap of the TN cell. The apparent order parameter of LC layer in the TN cell is calculated using the measured birefringence of LC layer in the TN cell. The pretilt angle of LC molecules increases linearly to the tilt angle of the optic axis of the rubbed PI surface. Both the apparent order parameter of LC layer and the effective twist angle of LC molecules decreases as the pretilt angle of LC molecules increases.

ACKNOWLEDGEMENT

REFERENCES

1. P. Yeh and C. Gu, *Optics of liquid crystal displays* (John Wiley & Sons, Inc., New York, 2010), Chapter 2.
2. M. Jiao, Z. Ge, Q. Song, and S. T. Wu, "Alignment layer effects on thin liquid crystal cells," Appl. Phys. Lett. **92**, 061102 (2008).
3. K. Ichimura, Y. Suzuki, T. Seki, Y. Kawanishi, and K. Aoki, "Reversible alignment change of liquid crystals induced by photochromic molecular films, 2. Reversible alignment change of a nematic liquid crystal induced by pendent azobenzene groups-containing polymer thin films," Makromol. Chem., Rapid Commun. **10**, 5-8 (1989).
4. B. Jerome, "Surface effects and anchoring in liquid crystals," Rep. Prog. Phys. **54**, 391 (1991).
5. K. Ichimura, "Photoalignment of liquid-crystal systems," Chem. Rev. **100**, 1847-1874 (2000).
6. L. A. Goodman, J. T. McGinn, C. H. Anderson, and F. DiGeronimo, "Topography of obliquely evaporated silicon oxide films and its effect on liquid-crystal orientation," IEEE Trans. Electron Devices **24**, 795-804 (1977).
7. G. Roberts, *Langmuir-Blodgett Films* (Springer Science & Business Media, 2013), Chapter 7.
8. N. A. J. M. van Aerle, M. Barmentlo, and R. W. J. Hollering, "Effect of rubbing on the molecular orientation within polyimide orienting layers of liquid-crystal displays," J.

Appl. Phys. **74**, 3111-3120 (1993).
9. Y. Sato, K. Sato, and T. Uchida, "Relationship between rubbing strength and surface anchoring of nematic liquid crystal," Jpn. J. Appl. Phys. **31**, L579 (1992).
10. A. J. Pidduck, G. P. Bryan-Brown, S. Haslam, R. Bannister, I. Kitely, T. J. McMaster, and L. Boogaard, "Atomic force microscopy studies of rubbed polyimide surfaces used for liquid crystal alignment," J. Vac. Sci. Tech. A **14**, 1723-1728 (1996).
11. I. Hirosawa, "Method of characterizing rubbed polyimide film for liquid crystal display devices using reflection ellipsometry," Jpn. J. Appl. Phys. **35**, 5873-5875 (1996).
12. I. Hirosawa, H. Miyairi, T. Matsushita, and S. Saito, "The relation between pretilt angle of liquid crystal and optical anisotropy of alignment layer," Mol. Cryst. and Liq. Cryst. **368**, 565-571 (2001).
13. T. Sakai, K. Ishikawa, H. Takezoe, N. Matsuie, Y. Yamamoto, H. Ishii, Y. Ouchi, H. Oji, and K. Seki, "Surface orientation of main and side chains of polyimide alignment layer studied by near-edge X-ray absorption fine structure spectroscopy," J. Phys. Chem. B **105**, 9191-9195 (2001).
14. J. J. Ge, C. Y. Li, G. Xue, I. K. Mann, D. Zhang, S.-Y. Wang, F. W. Harris, S. Z. D. Cheng, S.-C. Hong, X. Zhuang, and Y. R. Shen, "Rubbing-induced molecular reorientation on an alignment surface of an aromatic polyimide containing cyanobiphenyl side chains," J. Am. Chem. Soc. **123**, 5768-5776 (2001).
15. D. S. Seo, K. Araya, N. Yoshida, M. Nishikawa, Y. Yabe, and S. Kobayashi, "Effect of the polymer tlit angle for generation of pretilt angle in nematic liquid crystal on rubbed polyimide surfaces," Jpn. J. Appl. Phys. **34**, 503-506 (1995).
16. K. H. Lyum, S. U. Park, S. M. Yang, H. K. Yoon, and S. Y. Kim, "Precise measurement of ultra small retardation of LCD alignment layer using improved transmission ellipso- metry," Korean J. Opt. Photonics **24**, 77-85 (2013).
17. K. H. Lyum, H. K. Yoon, S. J. Kim, S. H. An, and S. Y. Kim, "Study of ultra-small optical anisotropy profile of rubbed polyimide film by using transmission ellipsometry," J. Opt. Soc. Korea **18**, 156-161 (2014).
18. J. H. Lee, M. S. Park, S. M. Yang, S. U. Park, M. H. Lee, and S. Y. Kim, "Precise measurement of the ultrasmall optical anisotropy of rubbed polyimide using an improved reflection ellipsometer," Korean J. Opt. Photonics **26**, 195-202 (2015).
19. M. S. Park, S. M. Yang, S. U. Park, and S. Y. Kim, "Quantitative characterization of uniaxial anisotropy of rubbed polyimide alignment layer using reflection ellipsometry," in *Proc. 22nd International Display Workshops* (Japan, Dec. 2015), pp. 68-69.
20. Retrieved from the world wide web; http://www.ellipsotech.com/Ellipsometer.html.
21. J. W. Ryu, *Study on the non-uniform distribution of anisotropy in wide view film using ellipsometry*, Ph.D. Dissertation, Ajou University, 36-113 (2010).
22. J. W. Ryu and S. Y. Kim, "Determination of the optic axis distribution of a hybridly aligned discotic material for wide-view films," J. Kor. Phys. Soc. **57**, 233-239 (2010).
23. S. Y. Kim, *Ellipsometry* (Ajou University Press, Korea, 2000), Chapter 3-4.

24. H. Fujiwara, *Spectroscopic ellipsometry: principles and applications* (John Wiley & Sons, Ltd., Japan, 2007).

25. S. Y. Kim, "Ellipsometric expressions of multilayered substrate coated with a uniaxially anisotropic alignment layer," Korean J. Opt. Photonics **24**, 271-278 (2013).

26. S. Y. Kim, "Ellipsometric expressions for a sample coated with uniaxially anisotropic layers," Korean J. Opt. Photonics **26**, 275-282 (2015).

27. S. Y. Cho, S. U. Park, and S. Y. Kim, "Quantitative characterization of optical anisotropy of rubbed polyimide alignment layers in relation with distribution of liquid crystal molecules using an improved reflection ellipsometer," in *Proc. 7th International Conference on Spectroscopic Ellipsometry* (Germany, Jun. 2016), p. 322.

28. S. Y. Cho, S. U. Park, S. M. Yang, and S. Y. Kim, "Ellipsometric characterization of the surface of rubbed polyimide and distribution of liquid crystal molecules in TN cells," in *Proc. 23rd International Display Workshops in Conjunction with Asia Display* (Japan, Dec. 2016), pp. 159-161.

29. P. G. de Gennes, "Short range order effects in the isotropic phase of nematics and cholesterics," Mol. Cryst. Liq. Cryst. **12**, 193-214 (1971).

30. V. G. K. M. Pisipati, D. Madhavi Latha, P. V. Datta Prasad, and G. Padmaja Rani, "Order parameter studies from effective order geometry in a number of liquid crystals of different homologous series," J. Mol. Liq. **174**, 1-4 (2012).

31. S. Patari, T. K. Devi, and A. Nath, "Studies of optical texture, birefringence, order parameter, normalized polarizability and validation of the four-parameter model of a thermotropic mesogen 7OAOB," J. Mol. Liq. **215**, 244-252 (2016).

32. M. F. Vuks, "Determination of the optical anisotropy of aromatic molecules from the double refraction of crystals," Opt. Spectrosc. **20**, 361-364 (1966).

33. A. Kanwar, "Measurement of order parameter, birefringence and polarizability of liquid crystals," J. Opt. **42**, 311-315 (2013).

34. S. Y. Kim, "The explicitly quasi-linear relation between the order parameter and normalized birefringence of aligned uniaxially anisotropic molecules determined using a numerical method," Korean J. Opt. Photonics **27**, 223 (2016).

35. S. Y. Kim, "Universality of the quasi-linear relation between the order parameter and the normalized birefringence of aligned uniaxially anisotropic molecules," Korean J. Opt. Photonics **28**, 33 (2017).